Switching behavior of individual pseudo-spin-valve ring structures

T. J. Hayward, J. Llandro, R. B. Balsod, and J. A. C. Bland
Cavendish Laboratory, University of Cambridge, Cambridge CB3 0HE, United Kingdom

D. Morecroft, F. J. Castaño, and C. A. Ross
Department of Materials Science and Engineering, Massachusetts Institute of Technology, Cambridge, Massachusetts 02139, USA
(Received 7 May 2006; revised manuscript received 27 July 2006; published 9 October 2006)

In this work, focused magneto-optic Kerr-effect magnetometry, magnetoresistance measurements, and three-dimensional micromagnetic simulations are combined to build a detailed picture of the magnetic switching behavior of micron-scale pseudo-spin-valve ring elements. We find that the reversal of the ring magnetization is dominated by the magnetostatic interaction of the higher magnetic-moment cobalt layer, which nucleates reverse domains in the NiFe free layer, causing it to switch in a manner that would not be possible in a single-layer ring. Measuring single pseudo-spin-valve rings has allowed the resolution of fine details in hysteresis loops, so that small differences between the magnetic states and switching of nominally identical elements can be observed. Furthermore, the high signal to noise ratio of the magnetoresistance measurements allows single-switching events to be observed in the structures. Using this technique we observe a range of phenomena involving both stable and metastable configurations of the ring, which would have been obscured in field-cycle-averaged data.

DOI: 10.1103/PhysRevB.74.134405 PACS number(s): 75.75.+a, 85.80.Jm, 75.70.Kw

I. INTRODUCTION

Micron-scale ferromagnetic ring-shaped structures have recently received much interest due to their suitability for use in magnetoelectronic devices such as magnetic random-access memory (MRAM) cells[1] and high-sensitivity magnetic sensors.[2] The magnetic states and switching behavior of such elements have been well characterized by a range of experimental techniques,[3–6] and the geometry has also provided an excellent test bed on which to examine the properties of geometrically constrained domain walls,[7,8] which are easily and reproducibly created by saturating the ring. So far the majority of work has focused on elements consisting of a single magnetic layer. However, for a viable MRAM or sensor device it is likely that a giant magnetoresistive (GMR) layer configuration, consisting of at least two ferromagnetic layers separated by a nonmagnetic spacer, would be required to increase the size of the available signal. Currently, only magnetoresistive (MR) measurements and micromagnetic simulations[9–12] have been used to study the switching of such pseudo-spin-valve (PSV) rings. While revealing the basic behavior of such a system, this approach is not suitable for investigating a wide range of ring geometries and layer sequences. The switching of PSV ring elements is also of interest because the interlayer magnetostatic interaction between domain walls has been shown to be highly important in the magnetic reversal process of multilayer magnetic films and elements.[13–15] The ease with which domain walls may be repeatedly formed in the ring geometry makes it an ideal system in which to study such effects in detail.

Here the results of focused magneto-optic Kerr effect (FMOKE) magnetometry,[16] magnetoresistance measurements, and three-dimensional (3D) micromagnetic simulations are combined to build a detailed picture of the magnetic switching behavior of micron-scale PSV ring elements. The FMOKE magnetometer allows hysteresis loops to be measured from single elements, and hence allows one to examine how the magnetic switching varies from one ring to another. The ability of the setup to measure single rings also means that it can resolve fine details in the hysteresis loop that would be obscured by the averaging inherent in conventional array-based MOKE magnetometry. Magnetoresistance measurements allow data from single reversal events to be obtained with high signal-to-noise ratios, so that variations in the switching from one applied field cycle to the next may be observed. Micromagnetic simulations give detailed information about the magnetic states and switching processes via which a nominally perfect ring would reverse its magnetization and act as a reference point from which to understand the fine details in the experimental data. Using these three techniques together allows an extremely thorough study of the switching of multilayer ring elements which surpasses that possible using a single technique alone.

II. EXPERIMENTAL METHODS

Arrays of polycrystalline PSV rings for FMOKE measurement [Fig. 1(a)] were fabricated on oxidized Si(001) using *e*-beam lithography and lift-off processing. The PSV layer configuration was Ti(8 nm)/Co(8 nm)/Cu(6 nm)/NiFe(6 nm)/Cu(3 nm). Un-

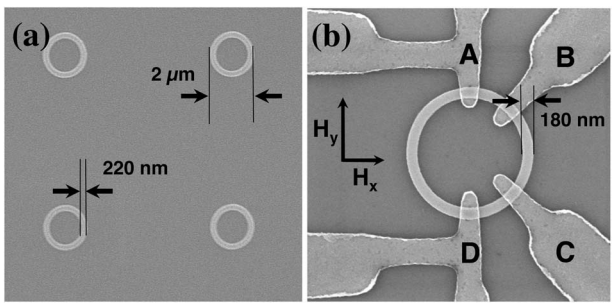

FIG. 1. SEM images of PSV ring structures with and without electrical contacts.

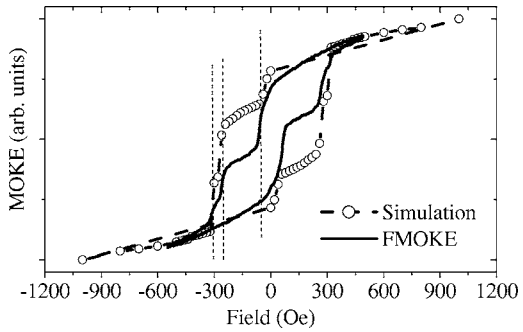

FIG. 2. Simulation (open circles) and FMOKE measurement (unbroken line) of the hysteresis loop of a 2-μm-diam, 220-nm-wide PSV ring structure.

patterned PSV films were polycrystalline with typical grain sizes of 10 nm. The rings had outer diameters of approximately 2 μm and widths between 200 and 450 nm. To minimize the interaction between the rings, the center-to-center spacing was maintained at approximately 8 μm. Further rings with a similar layer configuration [NiFe(4 nm)/Cu(5 nm)/Co(7 nm)/Au(4 nm)] were fabricated with four or six electrical contacts for magnetoresistance measurements [Fig. 1(b)].

Hysteresis loops of single rings were measured using a FMOKE magnetometer in which the probing laser spot was focused to $\sim$4 μm by a weak objective lens. The system used a 30 mW helium-neon laser stabilized to $<$0.1% rms noise by an external photoelastic modulator, which was also used to attenuate the incident laser power by a factor of 2. AC magnetic fields were applied by an external electromagnet with a maximum amplitude of 800 Oe.

MR measurements were made using a four-point contact geometry where a 90 μA-dc-sense current was injected through contacts A and D, while the voltage was measured across contacts B & C [Fig. 1(b)]. The level of the resistance detected is determined by the relative orientations of the magnetization vectors in the two magnetic layers.[17] The field was applied in two directions, H_x and H_y, so that the reversal in different sections of the ring could be explored in detail.[11] All measurements were carried out at room temperature.

3D micromagnetic simulations were carried out using the freely available OOMMF software.[18] The ring was discretized into 5 nm$\times$5 nm$\times$3 nm cells for which the direction of the magnetocrystalline anisotropy was randomly orientated to simulate the polycrystalline nature of the sample. The layer configuration differed slightly from that in the experimental arrays in that the thickness of the cobalt layer was increased from 8 nm to 9 nm, as the software did not allow inhomogeneous cell sizes to be used in the mesh. Standard parameters were used to characterize the properties of the Permalloy (exchange constant $A=13\times10^{-12}$ J m^{-1}, saturation moment $M_s=860\times10^3$ A m^{-1}, anisotropy $K_1=0$) and cobalt (exchange constant $A=30\times10^{-12}$ J m^{-1}, saturation moment $M_s=1400\times10^3$ A m^{-1}, anisotropy $K_1=520\times10^3$ J m^{-3}) layers. The thick Cu spacer layer suppresses exchange coupling between the ferromagnetic layers[19] and hence the RKKY interaction was ignored, leaving only the magnetostatic interaction between the layers. The simulation stepped the field in a quasistatic manner and the magnetization was allowed to evolve following the Landau-Lifschitz-Gilbert equation of motion so that a stable configuration was found at each field step applied between positive and negative saturation.

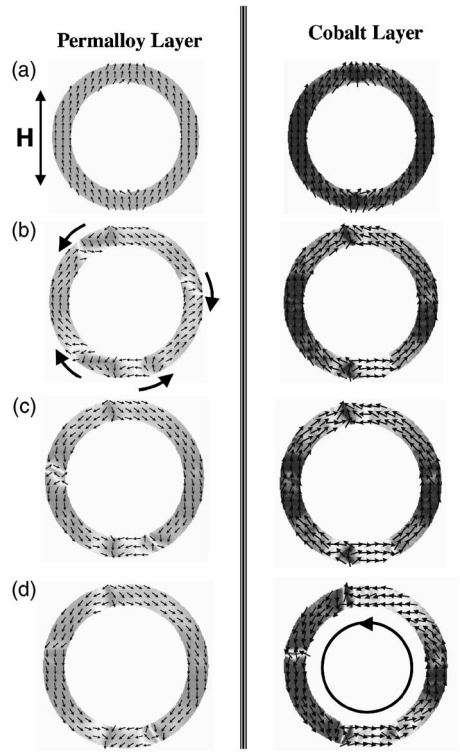

FIG. 3. Selected micromagnetic configurations for the soft (Permalloy) and hard (cobalt) layers in a 2-μm-diam PSV ring structure. Configurations are shown for applied fields values (a) 1 kOe, (b), 0 Oe, (c) −60 Oe, and (d) −280 Oe.

III. RESULTS AND DISCUSSION

Figure 2 shows a comparison between a FMOKE hysteresis loop measured from a single 220-nm-wide ring and a 3D micromagnetic simulation of the same structure. Both loops display a dominant two-step reversal in which the second step is broken by a small plateau. By comparing the hysteresis loop from an unpatterned film with the FMOKE data, the first transition was assigned to the Permalloy layer and the second transition to the reversal of the cobalt layer. The steps corresponding to the switching of the cobalt and Permalloy layers are different sizes in the simulation and FMOKE data because the MOKE response is not only controlled by the magnetization of the layer, but also by other factors such as the depth of the layer within the stack and the angle of the analyzing polarizer in the MOKE apparatus. Despite this, it is clear that the switching fields from the simulation and the experimental data are in excellent agreement, suggesting that the simulation is a good representation of the switching mechanisms that occur in the ring.

Figure 3 shows selected magnetic configurations from the simulated reversal of the ring. At the high positive field, both layers lie in aligned onion[20] states identical to those shown by thin single-layer rings [Fig. 3(a)]. As the applied field is

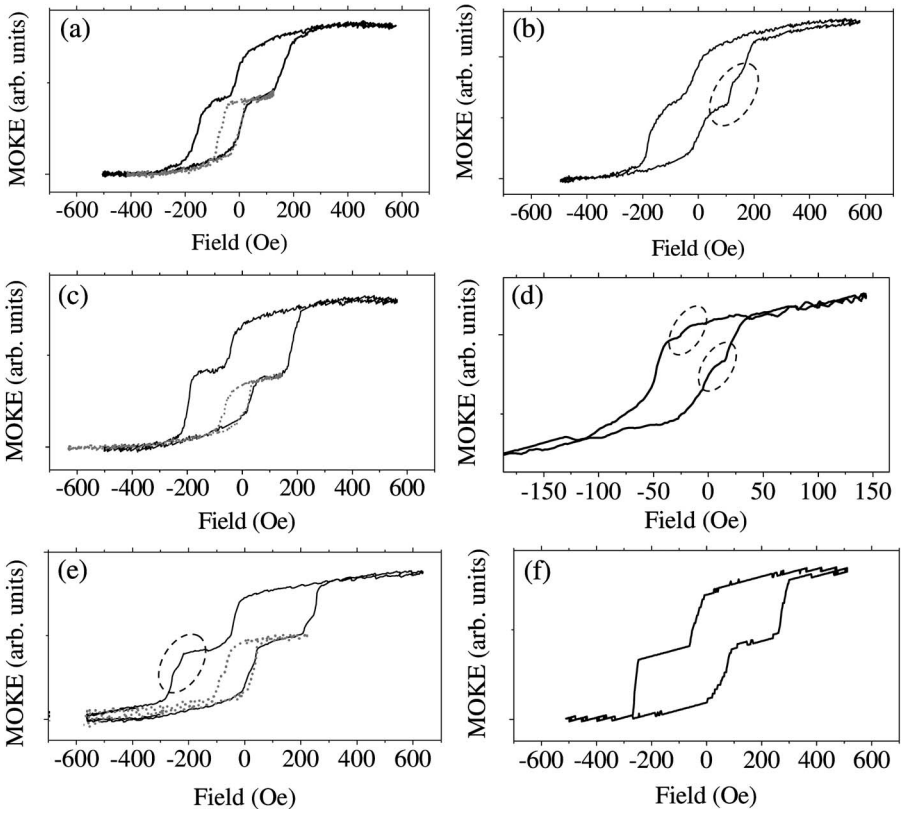

FIG. 4. FMOKE hysteresis loops measured from PSV ring structures with widths 450 nm (a and b), 300 nm (c and d), and 220 nm (e and f). For loops (a), (c), and (e) the minor loop created by reversing only the NiFe layer is shown with a dotted line, while (d) shows a much more detailed view of the minor loop from a 300-nm-wide ring in which plateaus corresponding to metastable configurations are highlighted. Small plateaus corresponding to the formation of a vortex state in the cobalt layer are also highlighted in (b) and (e).

reduced, the stray field from the domain walls in the cobalt layer causes the nucleation of two reverse domains in the Permalloy layer at the top and bottom of the ring [Fig. 3(b)], resulting in the formation of two pairs of domain walls which continue to sweep through the Permalloy layer as the field becomes negative. These domain walls pin in several metastable asymmetric configurations, suggesting that the reversal of the Permalloy layer is initially gradual with respect to the magnitude of the applied field and is likely to consist of many small jumps of magnetization as the combination of the applied field and the stray field of the cobalt layer overcomes the pinning of the domain walls by localized defects. Eventually the Permalloy layer is left in an onion state, which contains two 360° domain walls formed when the two pairs of 180° walls collide, but do not annihilate[21] [Fig. 3(c)]. The reversal of the Permalloy layer is consistent with that which was previously simulated for the reversal of a PSV elliptical ring of similar dimensions.[12] At this point the cobalt layer remains almost unaffected by the reverse field, aside from a slight twisting of spins in the left and right sides of the ring and a small disturbance at the bottom right, caused by the stray field from the walls in the Permalloy layer. This antiparallel configuration corresponds to the large plateau in the hysteresis loop. It also appears that the new 180° domain walls at the top and bottom of the Permalloy layer are aligned almost directly above those in the cobalt layer. This is likely to occur because, in this configuration, some flux closure is possible between the pairs of walls, lowering the magnetostatic energy. As the field becomes more negative, the twisting of the spins in the left-hand side of the cobalt layer becomes more pronounced, until an abrupt transition involving nucleation at the edges of the ring occurs, which completes the magnetization reversal of the left-hand side, leaving the cobalt layer in a vortex configuration [Fig. 3(d)] (although several 360° walls are also present within the vortex). This configuration is stable for a small range of fields until finally the right side reverses its magnetization via the same mechanism, returning the system to an aligned onion configuration. The small field range over which the cobalt vortex remains stable creates the smaller plateau in the hysteresis loop.

The simulation and FMOKE data show that there are two main features of interest in the reversal of the PSV. Firstly, the reversal of the Permalloy layer is unlike that shown by an isolated ring and appears to be a delicately balanced process as evidenced by the softness of the initial part of the Permalloy transition in the FMOKE loop, and the many metastable configurations shown by the magnetization in the simulation. Secondly, the vortex in the cobalt layer is not formed by the "classic" onion-to-vortex mechanism,[20] in which one head-to-head domain wall sweeps around the ring to annihilate with another. Instead, the domain walls appear to be pinned tightly so that the reversal of each side of the ring has to occur via a twisting of spins similar to that which is observed when a vortex state is eliminated. This equivalence of the reversal mechanism in both sides of the ring leads to an

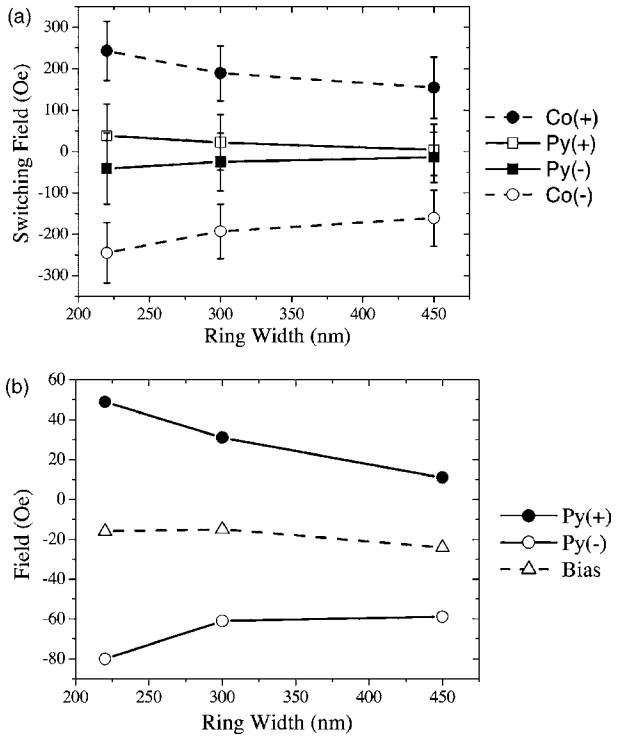

FIG. 5. Variation of switching field with ring width measured from the (a) major and (b) minor hysteresis loops of the PSV ring arrays. The error bars in (a) represent the FWHM of the switching-field distributions. (b) was measured by switching only the Permalloy layer in the rings and also shows the variation of the offset in the hysteresis loop caused by the magnetostatic interaction of the cobalt layer.

extremely low stability of the vortex state, as both sides switch by the same mechanism and therefore their reversal processes will be governed by energy barriers of similar magnitude. It is also of note that the features of the cobalt-layer reversal are of different origin than those of the Permalloy layer. The behavior of the Permalloy layer is dominated by the interaction with the cobalt layer's domain walls beneath it, whereas the low-field range over which the cobalt layer's vortex state is present is similar to that which has been reported for single-layer Co rings of a similar thickness.[22]

To study the features described above further, a series of PSV rings with widths 220, 300, and 450 nm were measured using the FMOKE magnetometer. For each width a large number of individual rings were measured so that a broader understanding of the switching processes occurring could be gained. A selection of the hysteresis loops obtained are shown in Fig. 4. For all of the rings measured, the dominant two-stepped behavior was evident; however, only a selection of the rings showed a clear vortex state in the reversal of the cobalt layer, as may be observed by comparing Fig. 4(a) with Fig. 4(b) and Fig. 4(e) with Fig. 4(f). The proportion of rings that displayed a Co vortex increased from 40% in the widest rings to 70% in the narrowest, suggesting that the question of whether a vortex state forms may be dictated by shape irregularities, which are more likely to have a significant effect in the more narrow rings, delaying the transition in one half of the ring. However, it is also important to note that the formation of a vortex in the cobalt layer may be influenced by other factors such as the stray field from the head-to-head domain walls of the cobalt or Permalloy layers, which are asymmetrically pinned in the simulation. The average field range over which the vortex state was present was 45 Oe for all widths. A further point of interest is that the abruptness of the transitions increases as the width decreases. This is likely to be due to fact that the lower-width rings constrain the spins more tightly so that less reversible twisting of the magnetic configuration may occur.

Figure 4(d) presents a minor loop produced by switching the Permalloy layer back and forth over a cobalt onion state in a 300-nm-wide ring. As expected from the simulation, and as observed in elliptical PSV rings,[12] the minor loop shows several small plateaus (highlighted in the figure), corresponding to metastable configurations of the layer. The exact shape of the minor loop varied from ring to ring indicating that small differences in the structure can change the configurations that the free layer passes through during a reversal. The minor loop also shows a shift of approximately −20 Oe from the zero field due to the interaction of the cobalt layer's magnetostatic field, which favors the antiparallel alignment.

In order to characterize the average behavior of the rings, the FMOKE magnetometer laser spot was defocused so that it could simultaneously measure a large portion of the ring array in the manner of a conventional MOKE system. Figure 5(a) shows how the average switching fields of the two layers varied with the width of the ring. The vortex state was not resolved in these loops and hence there is only a single transition measured for each reversal of the cobalt layer. The data indicates that the field required to switch the magnetization of the layers increases when the width of the ring decreases. This can be understood by considering the behavior of a single-layer ring: the Permalloy layer switches via domain-wall propagation in a manner similar to the onion-to-vortex transition in single-layer rings. Lowering the width of the ring increases the effect that edge defects have on the reversal and also shortens the domain wall, so that pinning is stronger at both intrinsic and extrinsic imperfections, increasing the switching field. The cobalt-layer reversal is initiated by a twisting of spins in the sides of the ring in the same way that the vortex-to-onion transition is initiated in single-layer rings. If the width of the ring decreases, the spins are more tightly aligned to a circumferential configuration, delaying the onset of the transition with respect to the magnitude of the applied field. The error bars on the graph represent the switching-field distributions (full width at half maximum) measured from the hysteresis loops. For all the observed transitions the size of the distribution lies in the range 60–85 Oe. For the Permalloy layer the distribution increases slightly with decreasing width, whereas for the cobalt layer the distributions stay approximately the same size. This is as expected, as the domain-wall motion switching of the Permalloy layer is likely to be much more susceptible to edge roughness than the transition of the cobalt layer.

Figure 5(b) shows how the switching fields measured from the minor loop of the Permalloy layer vary with the width of the ring. The offset of the loop caused by the mag-

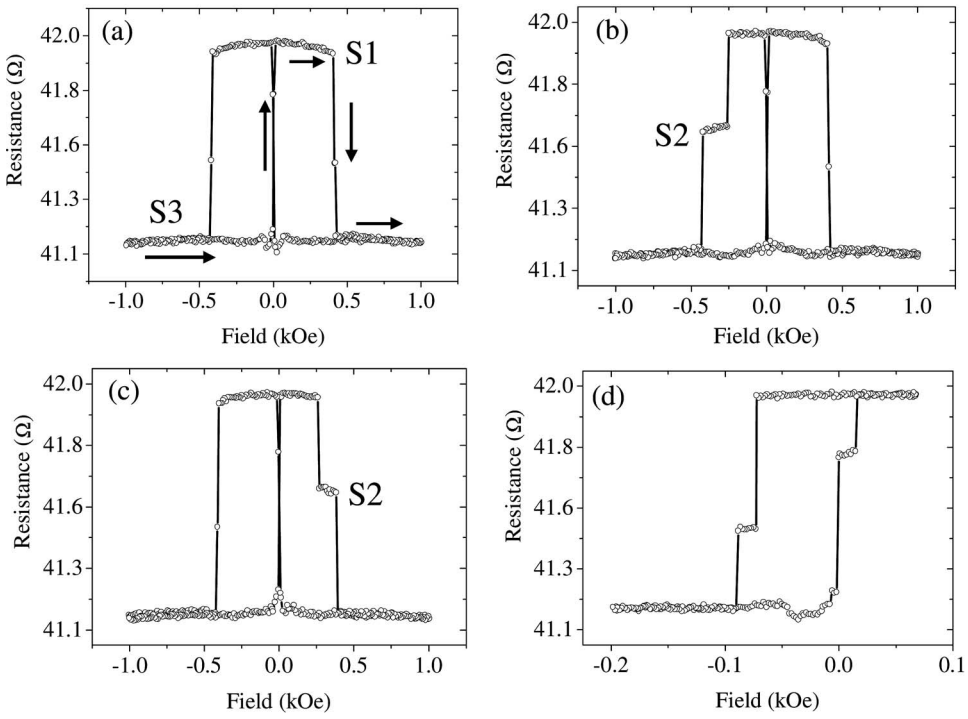

FIG. 6. Single-field-cycle magnetoresistance data measured from a 2-μm-ring device with the field orientated in direction H_y. (a), (b), and (c) show major loops while (d) shows a minor loop from cycling only the NiFe layer.

netostatic interaction of the cobalt layer is also shown, and was found to be ~ -20 Oe for all rings, while decreasing weakly with ring width. This suggests that the total saturation moment of the cobalt layer may be the dominating factor in determining the interlayer interaction rather than the spin configuration itself, as at lower widths the transverse walls would be expected to show larger spin components perpendicular to the edge of the ring creating the potential for a higher stray field. It is also possible that the lower-ring width introduces changes in the spin configuration of the Permalloy layer that make it less effectively biased by the cobalt layer interaction.

While the MOKE measurements provide information on the switching of nominally identical magnetic elements, they revealed little about the cycle-to-cycle variability shown by the rings. To investigate this, magnetoresistance measurements were used to probe single-switching events in a 2 -μm-diam PSV ring of width 180 nm. Figure 6(a) shows a single-field-cycle MR curve measured with the field applied in the direction labeled H_y in Fig. 1(b). At negative saturation the two magnetic layers are well aligned and hence a low resistance level $S3$ is recorded. At a small reverse field the Permalloy layer is reversed leading to an antiparallel alignment and a higher resistance level $S1$. Finally, at a much higher reverse field the cobalt layer also switches to align with the field returning the resistance level to $S3$. With an applied-field amplitude of 1 kOe it was found that, in some loops, a third resistance level $S2$ occurred, corresponding to the formation of a vortex state in the cobalt layer [Figs. 6(b) and 6(c)], although this reversal path was much less common than the two-step reversal. The stability range of the vortex state was found to be >150 Oe, which is a much larger field range than that corresponding to range of stability of vortex states measured in the FMOKE data. It was also found that, while the final transition back to $S1$ occurred at approximately the same field whether or not a vortex was formed, the transition into the vortex state occurred at a much lower field value, suggesting that a different mechanism from that involved in the single-step switching caused such a transition. The likely implication of this is that, in reversals where a vortex state was observed, the domain walls of the cobalt layer had been left in a configuration where they were less tightly pinned and hence formed a vortex state by domain-wall motion and annihilation. The vortex is stable over a larger range of fields than was observed in the FMOKE data because the mechanisms of vortex formation and annihilation are now different, rather than similar as they were found to be in the simulation. When the applied-field amplitude was increased to 2 kOe, vortex states with a large-field stability range were no longer observed, suggesting that by saturating the rings further, and hence exerting tighter control of the magnetization history of the ring, the switching could be regulated. It is likely that the domain walls of the cobalt layer were pushed to a more symmetric configuration by the higher applied field making it harder for a reverse field to exert a torque on them.

Figure 6(d) shows an example of a minor loop measured by switching only the Permalloy layer of the PSV device. The loop clearly shows that stable intermediate states are formed in the switching of the layer magnetization. These intermediate states were found to be reproducibly created over many-field cycles and are likely to be similar to those responsible for the small plateaus observed in the FMOKE minor loop [Fig. 4(d)].

When the field orientation was changed to H_x the contact configuration was highly sensitive to the alignment of the

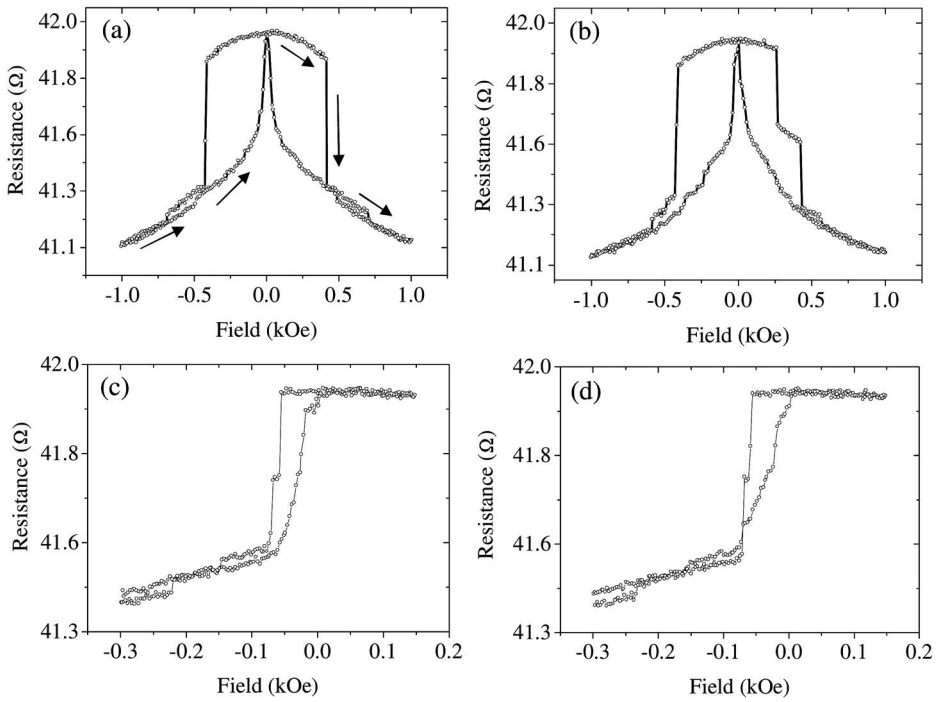

FIG. 7. Single-field-cycle magnetoresistance data measured from a 2-μm-ring device with the field orientated in direction H_x. (a) and (b) show major loops while (c) and (d) show minor loops from cycling only the NiFe layer.

magnetic layers in the right-hand side of the ring, and therefore to the nucleation and motion of the domain walls in the Permalloy layer.[11] Figures 7(a) and 7(b) show example single-reversal MR curves produced with the field in this orientation. The sweeping of the Permalloy layers' domain walls through the ring, which was predicted by the simulation, can be clearly observed in the gradual increase of the resistance level as the ring is relaxed towards remanence. Figures 7(c) and 7(d) show minor loops produced with the same field orientation. The reversal path in the forward-field direction is slightly different in the two cases, showing that the motion of the domain walls varies from cycle to cycle, most likely due to a combination of localized pinning and the intrinsic sensitivity of a system involving a large number of interacting domain walls. However, the reverse transition is much better defined and was virtually identical in all the reversals observed. By considering this data along with the minor loops taken in the H_y field orientation it is clear that, while there is cycle-to-cycle variability in the reversal of the Permalloy layer, the final, abrupt parts of the transition are well defined, a feature which is highly important for a magnetoelectronic device. The reverse-field sweep also produced abrupt changes in the resistance for both field orientations, suggesting that a gradual reversal of the Permalloy layer only occurs when the switching is aided by the magnetostatic field of the cobalt layer.

IV. CONCLUSIONS

By combining FMOKE and magnetoresistance measurements with the results of 3D micromagnetic simulations, a detailed picture of the reversal processes occurring in micron-scale pseudo-spin-valve ring devices has been obtained. Some features of the reversal were found to be similar to those occurring in an isolated ring, while others, such as the reversal of the Permalloy free layer are altered significantly by the interaction between the layers. The reversal mechanism of the ring is dominated by the behavior of the higher-moment cobalt layer, which changes the switching mechanism of the Permalloy layer from that of a single-layer ring, while the cobalt layer's own switching mechanism is the same as might be expected in a single-layer ring of similar thickness.

By measuring a number of rings individually, we have found that for a given ring geometry a variety of different reversal paths may occur during the switching of nominally identical rings. This is most likely due to small-scale differences between the rings in an array, such as edge roughness. We have also observed changes in the switching of an individual ring from one field cycle to the next, including variations of both the stable and metastable states through which the ring passes. The switching repeatability of the rings was found to be improved by the use of a higher saturation field, suggesting that the magnetization history plays an important role in dictating the reversal path of the rings, in addition to intrinsic variability due to the thermally activated depinning of the magnetic configurations at defects. Control of the switching variability will be important for such structures to be effectively integrated as magnetoelectronic devices.

ACKNOWLEDGMENTS

The authors are grateful for the support of the Cambridge-MIT Institute (CMI) and the Engineering and Physical Sciences Research Council (EPSRC).

[1] X. Zhu and J.-G. Zhu, IEEE Trans. Magn. **39, 5**, 2854 (2003).
[2] M. M. Miller, G. A. Prinz, S.-F. Cheng, and S. Bounnak, Appl. Phys. Lett. **81**, 2211 (2002).
[3] M. Kläui, C. A. F. Vaz, J. A. C. Bland, T. L. Monchesky, J. Unguris, E. Bauer, S. Cherifi, S. Heun, A. Locatelli, L. J. Heyderman, and Z. Cui, Phys. Rev. B **68**, 134426 (2003).
[4] M Kläui, C. A. F Vaz, L. Lopez-Diaz, and J. A. C. Bland, J. Phys.: Condens. Matter **15**, R985 (2003).
[5] F. Giesen, J. Podbielski, T. Korn, and D. Grundler, J. Appl. Phys. **97**, 10A712 (2005).
[6] M. Steiner and J. Nitta, Appl. Phys. Lett. **84**, 939 (2004).
[7] R. D. McMichael and M. J. Donahue, IEEE Trans. Magn. **33**, 4167 (1997).
[8] M. Kläui, C. A. F. Vaz, J. A. C. Bland, W. Wernsdorfer, G. Faini, E. Cambril, L. J. Heyderman, F. Nolting, and U. Rudiger, Phys. Rev. Lett. **94**, 106601 (2005).
[9] N. Dao and S. L. Whittenburg, IEEE Trans. Magn. **39**, 2525 (2003).
[10] D. Morecroft, F. J. Castaño, W. Jung, J. Feuchtwanger, and C. A. Ross, Appl. Phys. Lett. **88**, 172508 (2006).
[11] D. Morecroft, F. J. Castaño, W. Jung, and C. A. Ross, J. Appl. Phys. **99**, 08T104 (2006).
[12] F. J. Castaño, D. Morecroft, W. Jung, and C. A. Ross, Phys. Rev. Lett. **95**, 137201 (2005).
[13] H. W. Fuller and D. L. Sullivan, J. Appl. Phys. **33**, 1063 (1962).
[14] L. Thomas, M. G. Samant, and S. S. P. Parkin, Phys. Rev. Lett. **84**, 1816 (2000).
[15] W. S. Lew, S. P. Li, L. Lopez-Diaz, D. C. Hatton, and J. A. C. Bland, Phys. Rev. Lett. **90**, 217201–1 (2003).
[16] D. A. Allwood, G. Xiong, M. D. Cooke, and R. P. Cowburn, J. Phys. D **36**, 2175 (2003).
[17] J. A. C. Bland and B. Heinrich, *Ultrathin Magnetic Structures III* (Springer, New York, 2005).
[18] OOMMF software package, M. Donahue and D. Porter, http://math.nist.gov/oommf
[19] D. Lottis, A. Fert, R. Morel, L. G. Pereira, J. C. Jacquet, P. Galtier, J. M. Coutellier, and T. Valet, J. Appl. Phys. **73**, 5515 (1993).
[20] J. Rothman, M. Kläui, L. Lopez-Diaz, C. A. F. Vaz, A. Bleloch, J. A. C. Bland, Z. Cui, and R. Speaks, Phys. Rev. Lett. **86**, 1098 (2001).
[21] F. J. Castaño, C. A. Ross, C. Frandsen, A. Eilez, D. Gil, H. I. Smith, M. Redjdal, and F. B. Humphrey, Phys. Rev. B **67**, 184425 (2003).
[22] Y. G. Yoo, M. Kläui, C. A. F. Vaz, L. J. Heyderman, and J. A. C. Bland, Appl. Phys. Lett. **82**, 2470 (2003).